Mathematical Geology, Vol. 32, No. 6, 2000

The FFT Moving Average (FFT-MA) Generator: An Efficient Numerical Method for Generating and Conditioning Gaussian Simulations[1]

Mickaële Le Ravalec,[2] Benoît Noetinger,[2] and Lin Y. Hu[2]

A fast Fourier transform (FFT) moving average (FFT-MA) method for generating Gaussian stochastic processes is derived. Using discrete Fourier transforms makes the calculations easy and fast so that large random fields can be produced. On the other hand, the basic moving average frame allows us to uncouple the random numbers from the structural parameters (mean, variance, correlation length, . . .), but also to draw the randomness components in spatial domain. Such features impart great flexibility to the FFT-MA generator. For instance, changing only the random numbers gives distinct realizations all having the same covariance function. Similarly, several realizations can be built from the same random number set, but from different structural parameters. Integrating the FFT-MA generator into an optimization procedure provides a tool theoretically capable to determine the random numbers identifying the Gaussian field as well as the structural parameters from dynamic data. Moreover, all or only some of the random numbers can be perturbed so that realizations produced using the FFT-MA generator can be locally updated through an optimization process.

KEY WORDS: simulation, nonlinear conditioning, optimization, FFT, local perturbation.

INTRODUCTION

In reservoir engineering, we are interested in the modeling of transport properties such as permeability and porosity within a reservoir. As the true distribution of these properties is unknown, we assume that they can be approximated from Gaussian random fields or transforms of Gaussian random fields. In addition, those fields must be constrained to dynamic data such as well pressures, production history, and water cut. But the relations between dynamic data and permeability/porosity distributions are nonlinear, making conditioning very difficult so that an iterative solver is used. Then fluid flow simulations are performed for a large number of random fields representing permeability and/or porosity distributions to capture the range of possible dynamic behaviors. The set of alternative realizations provides

[1]Received 27 January 1999; accepted 18 August 1999.

[2]Institut Français du Pétrole, 2, av. du Président Pierre Angot, 64053 Pau Cedex 9 France. e-mail: mickaele.le-ravalec@ifp.fr

a measure of uncertainty about the spatial distribution of permeability/porosity values.

A traditional statistical method that produces Gaussian random fields is the Cholesky decomposition of the covariance matrix. Its main advantages are simplicity, ability to generate random numbers and achieve conditioning simultaneously (Davis, 1987; Alabert, 1987) and ability to handle any point location pattern. However it is restricted to moderate point numbers. When generating a random field over N points, covariance matrix dimensions are $N \times N$. The greater N, the less tractable the decomposition of the covariance matrix. Practically, the Cholesky decomposition method is limited to 1000 points. As it is of common practice in reservoir characterization for N to be of the order of 10^6, other methods need to be used.

The moving average method was developed to simulate one-dimensional Gaussian random fields with stationary covariances (e.g., Journel, 1974). Then, it was further extended by Oliver (1995) to two and three dimensions. This method is very similar to the Cholesky decomposition. The only difference depends on the decomposition technique. The moving average method requires that the covariance function is expressed as a convolution product of a function g and its transpose. In this case, it is no longer necessary to tackle the numerical decomposition of a large matrix. However, there is still an important difficulty: the computation of function g. Up to now, just a few particular covariance functions were investigated (Oliver, 1995).

There are several other approaches often referred in the literature to simulate random fields over a large number of points: the sequential Gaussian simulation (Johnson, 1987; Gomez-Hernandez and Journel, 1992), the turning bands (TUBA) method (Matheron, 1973; Mantoglou and Wilson, 1982), the continuous spectral method (Shinozuka and Jan, 1972; Lantuéjoul, 1994), and the discrete spectral method based on the fast Fourier transform (FFT) method (Gutjahr, 1989; Pardo-Iguzquiza and Chica-Olmo, 1993; Chilès, 1995). It is outside the scope of this paper to compare these approaches. To compare briefly: the TUBA and the continuous spectral method are limited to particular covariance functions, but can be applied to estimate random field values in any point of the reservoir (Blanc, Touati, and Hu, 1998). On the contrary, the FFT method produces stochastic processes having any kind of stationary covariance function, but only for equal-spaced gridding. Extensions have been developed to combine the advantages of the TUBA and FFT methods (Mantoglou, 1987).

Conditioning realizations to values measured at some locations is performed either straightforwardly or using a traditional approach based on kriging (Journel and Huijbregts, 1978). In this case, only linear relations are involved. However, forcing the realizations to honor dynamic data, such as well pressures, is a difficult task due to the nonlinear relations between the dynamic variables and the field values.

In this paper, we are going to focus on the use of the FFT algorithm because of its efficiency and its ability to produce large Gaussian random fields with stationary covariance functions. Using the same theoretical background, Gutjahr, Bullard, and Hatch (1997) suggested that simulated fields be conditioned with kriging either in the space or spectral domains. Yao (1998) built a different approach to avoid solving the kriging system. She assumed, as Pardo-Iguzquiza and Chica-Olmo (1993) did, that the amplitude of each spectral component of the random field equals its variance. As a result, the amplitude spectrum can no longer be random: it depends on the spectral density that is the Fourier transform of the covariance function. In this case, the phase spectrum does not affect the covariance structure: it is uniformly distributed between 0 and 2π. Then, Yao (1998) used the simulated annealing algorithm to constrain the phases of the Fourier coefficients of the random field realization.

This paper introduces a new generator for simulating Gaussian stationary stochastic processes. It is very consistent with the gradual deformation method (Hu, 2000) and turns out to be well suited to optimization problems. This generator, called the FFT moving average (FFT-MA) generator, results from the combination of the moving average method with the FFT algorithm. Because computations are carried out through FFTs, simulations are fast and stable. Contrary to the conventional spectral generator, the FFT-MA generator relies on randomness components drawn in spatial domain. This very distinctive feature, inherent in the moving average approach, allows us to perturb the simulated realizations locally. We detailed the implementation of the suggested algorithm in the first section, before focusing on its advantages. The last section is dedicated to the analysis of a synthetic example. We show how to take advantage of the FFT-MA generator to update a reservoir model integrating newly obtained data.

DESCRIPTION OF THE METHOD

Moving Average

As mentioned earlier by Oliver (1995), the scheme of the moving average method is pretty close to that of the Cholesky method. Let us recall briefly the basics of the Cholesky approach. First, using the Cholesky algorithm, the covariance matrix $\mathbf{C}$ is expressed as a product of upper and lower triangular matrices:

$$\mathbf{C} = \mathbf{L}\mathbf{L}^t \tag{1}$$

Matrix $\mathbf{L}$ is used to generate a Gaussian random field $\mathbf{y}$ with mean $\mathbf{m}$ and covariance matrix $\mathbf{C}$ from a vector $\mathbf{z}$ of uncorrelated random normal deviates distributed

as $N(0, I_N)$:

$$\mathbf{y} = \mathbf{m} + \mathbf{Lz} \tag{2}$$

When using the moving average method, we consider the n-dimensional covariance function C instead of the covariance matrix. This covariance operator is written as a convolution product of a function g and its transpose ($\check{g}(x) = g(-x)$):

$$C = g * \check{g} \tag{3}$$

If the n-dimensional function g can be calculated, a Gaussian random field y with mean m and covariance C is generated by the operation:

$$y = m + g * z \tag{4}$$

z is a n-dimensional field of uncorrelated normal deviates (also called "Gaussian white noise"). It forms a basic building block in the construction of more complicated realizations.

Both methods convolve normal deviates with a decomposition of the covariance. However, for the first one, the numerical decomposition of the covariance matrix is very computationally intensive for large fields. This size constraint is avoided when using the moving average method, but determining g can be a difficult task. For instance, the analytical calculation of g for a spherical covariance operator is an intractable problem in two dimensions (Oliver, 1995).

The FFT-MA Generator

For all these reasons, we decided to build a FFT-MA generator taking advantage of the moving average framework, but also of the discrete spectral calculations. Computing g turns out to be numerically unstable for some covariance functions. This calculation is no longer necessary when using the FFT-MA algorithm. The basic idea of this method is to determine the convolution product $g * z$ in the frequency domain.

First of all, we recap some properties associated to stationary random fields. The Bochner (1936) theorem states that any stationary process has a covariance function C of the form:

$$C(x) = \int_{-\infty}^{+\infty} S(f) \exp(2i\pi f \cdot x)\, df \tag{5}$$

S is the power spectrum or spectral density function: it depends on frequency f. The integral is an abbreviation for the n-fold integral where n is the dimension

of the space. The covariance and power spectrum functions provide the same information, but in different space. C is the inverse Fourier transform of S, while S is the forward Fourier transform of C. S can be expressed as

$$S(f) = \int_{-\infty}^{+\infty} C(x) \exp(-2i\pi f \cdot x)\, dx \tag{6}$$

The n-dimensional Fourier transform of a n-dimensional convolution is the product of the n-dimensional Fourier transforms of each convolved function, that is,

$$\mathcal{F}(g * h) = \mathcal{F}(g)\mathcal{F}(h) \tag{7}$$

As the covariance function is real and even, the power spectrum is real and even too. In addition, an important property of stationary processes is the orthogonality of their spectral components (Priestley, 1981). Let us denote Y the Fourier transform of $y - m$. The expectation of the variance of Y is

$$\begin{aligned} E[Y(f)\overline{Y(f')}] &= E[G(f)Z(f)\overline{G(f')Z(f')}] = G(f)\overline{G(f')}E[Z(f)\overline{Z(f')}] \\ &= \begin{cases} 0 & \text{if } f \neq f' \\ G(f)\overline{G(f)} = S(f) & \text{if } f = f' \end{cases} \end{aligned} \tag{8}$$

where G and Z are the Fourier transforms of g and z, respectively. This equality holds because z is a stationary random field with a dirac covariance measure (i.e., a Gaussian white noise). It ensures the positivity of $S(f)$.

One of the most fundamental results in the theory of stationary processes is that realizations are expressed not as Fourier transforms, but as Fourier–Stieltjes transforms. Within this framework, the definition of continuous random processes poses considerable problems. In fact, no such process exists, except in a highly degenerate sense (Priestley, 1981). Instead of developing a continuous approach as Oliver (1995), we prefer to focus on the discrete case in order to avoid that kind of difficulty. This is one of the reasons why we use the FFT approach. In addition, contrary to the continuous spectral method, it is unnecessary to determine the square root of the covariance function g. We only compute the Fourier transform of $g * z$.

All of the previous results can be rewritten within a discretized framework. For simplicity in notation, the development is presented in one dimension, but it extends easily to two and three dimensions.

Because using Fourier transforms implies periodicity, the desired field is oversized. Let us assume that we want to produce a stochastic process of size Ndx and N is the number of points and dx the sampling rate. Instead, we generate a

process of size $Ndx + l_c$, where l_c is the correlation length. After simulation, the additional points are discarded. Therefore, the first and last points of the sequence are uncorrelated.

Broadly speaking, we consider a sequence of N_1 equidistant points. The corresponding frequency rate is selected carefully so that there is no aliasing. If dx_1 is the sampling rate, the frequency rate is $df_1 = 1/(N_1 dx_1)$ and the frequency range $[-1/(2dx_1); 1/(2dx_1)]$. Symmetry properties imply

$$\begin{aligned} S(j_1) &= dx_1 \sum_{k_1=1}^{N_1} C(k_1) \exp\left(-2i\pi \frac{k_1 j_1}{N_1}\right) \\ C(k_1) &= \frac{1}{N_1 dx_1} \sum_{j_1=1}^{N_1} S(j_1) \exp\left(2i\pi \frac{k_1 j_1}{N_1}\right) \\ \mathcal{F}(g * h) &= \frac{1}{dx_1} \mathcal{F}(g)\mathcal{F}(h) \end{aligned} \tag{9}$$

The decomposition of the covariance operator is now straightforward. The discretized power spectrum S is derived from the discretized covariance function C. Equation (3) can be rewritten as

$$S(j_1) = \frac{1}{dx_1} G(j_1)\overline{G(j_1)} \tag{10}$$

The only requirement on function g is that Equation (3) is satisfied. As solutions to this equation are not unique, additional constraints are considered to get functions with particular forms (Oliver, 1995). In this case, G (hence g) is picked, so that

$$G(j_1) = \sqrt{dx_1 S(j_1)} \tag{11}$$

Such a decomposition, that is said to be symmetric, is appropriate because the Fourier transform of a convolution product is the product of Fourier transforms and because the power spectrum is real, positive and symmetric.

Implementation

To generate unconditional Gaussian random fields, we proceed according to seven steps.

1. Building of the sampled covariance C (Fig. 1).
2. Generation of the normal deviates z on the grid.
3. Calculation of the Fourier transforms of z and C, giving Z and the power spectrum S, respectively.

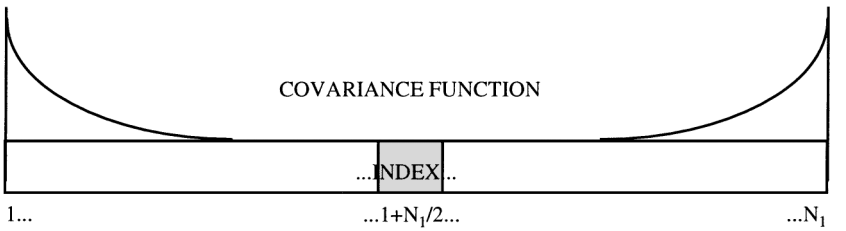

Figure 1. Sketch of the covariance sequence for a one-dimensional case.

4. Derivation of G from S.
5. Multiplication of G by Z.
6. Inverse Fourier transform of $(G \cdot Z)$ giving $g * z$.
7. Derivation of y from Equation (4).

The sampling of the covariance function must be performed cautiously so that the discrete covariance, hence the discrete power spectrum, are real and even. The length of the covariance sequence is the same as the length of the field to simulate. In the case of one-dimensional processes with N_1 points, the covariance sequence is $(C(k_1), k_1 = 1, N_1)$ with $k_1 = 1 + N_1/2$ characterizing the symmetry axis. The building rules are (Fig. 1)

1. $C(k_1)$ is associated to the distance $(k_1 - 1)\,dx_1$ when $k_1 \leq 1 + N_1/2$.
2. $C(k_1) = C(N_1 - k_1 + 1)$ if N_1 is odd and $k_1 > 1 + N_1/2$.
3. $C(k_1) = C(N_1 - k_1 + 2)$ if N_1 is even and $k_1 > 1 + N_1/2$.

Fourier transforms are computed using the Cooley-Tukey (1965) algorithm, which is more efficient when N_1 is a product of small prime factors. Thus, realizations are oversized to avoid the correlation effects due to periodicity as stated above, but also to avoid aliasing and to have dimensions that can be decomposed in small prime factors. After simulation, the unneeded cells are removed.

STRENGTHS OF THE METHOD

First, this method is fast and flexible. As discussed above, it can handle any permissible covariance as long as the field is stationary. Second, it is based on the convolution of the square root of the covariance function with a Gaussian white noise. That is: the structural parameters are separated from the random ones. Then, different realizations with all the same covariance can be produced running the simulation with the same square-root operator, but considering different normal deviates. In addition, the structural parameters (as the correlation length) can be also varied while keeping the same set of random numbers.

Computational Efficiency and Numerical Stability

In order to point out the efficiency of the method with fairly large fields, we perform a few runs over 200×200 grids (Figs. 2–4). The covariance models that we use are as follows for isotropic distributions:

Exponential model

$$C(h) = \sigma^2 \exp\left(-\frac{h}{l_c}\right)$$

Gaussian model

$$C(h) = \sigma^2 \exp\left(-\left(\frac{h}{l_c}\right)^2\right)$$

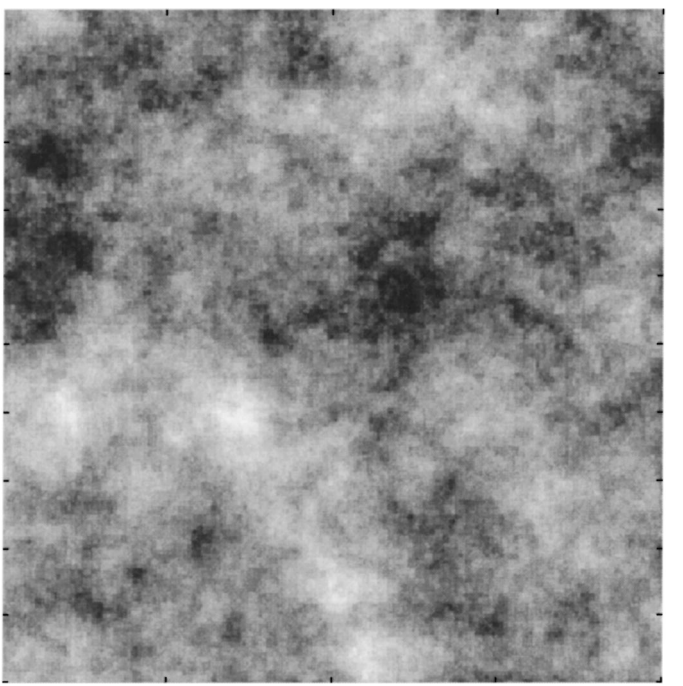

Figure 2. Two-dimensional isotropic Gaussian random field with exponential covariance (grid: 200×200 nodes; space step: 1; correlation length: 50; mean: 0; variance: 1).

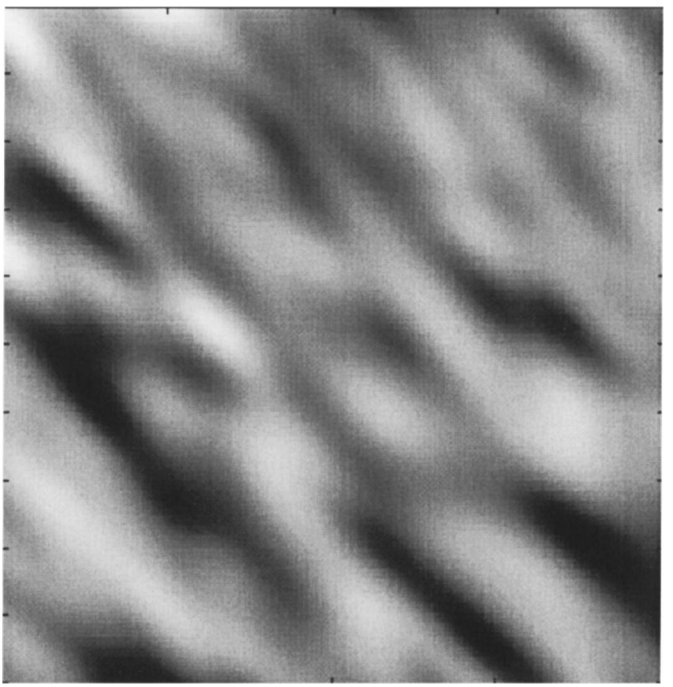

Figure 3. Two-dimensional anisotropic Gaussian random field with Gaussian covariance (grid: 200×200 nodes; space step: 1; major correlation length: 50; minor correlation length: 20; mean: 0; variance: 1).

Spherical model

$$\begin{aligned} C(h) &= \sigma^2\left(1 - \frac{3}{2}\frac{h}{l_c} + \frac{1}{2}\frac{h^3}{l_c^3}\right) && h \le l_c \\ &= 0 && h > l_c \end{aligned}$$

Stable model

$$C(h) = \sigma^2 \exp\left(-\left(\frac{h}{l_c}\right)^{\alpha}\right)$$

The h is the space lag, σ^2 is the variance and l_c is the correlation length. The α is an exponent ranging between 0 and 2. Actually, 100 realizations are built for all of these models. The results of the ensemble statistics are reported in Table 1. The general trend demonstrates a reasonable behavior. The means of means and variances are close to their theoretical values (0 and 1, respectively) and dispersion is small.

Table 1. Average Statistics of 100 Isotropic Two-Dimensional Realizations (Grid: 200 × 200 Nodes; Space Step: 1; Correlation Length: 50; Theoretical Mean: 0; Theoretical Variance: 1)

Covariance model	Mean of means	Variance of means	Mean of variances	Variance of variances
Exponential	$5.75\ 10^{-2}$	$3.79\ 10^{-2}$	0.97	$2.03\ 10^{-2}$
Gaussian	$2.47\ 10^{-2}$	$4.51\ 10^{-2}$	0.94	$4.60\ 10^{-2}$
Spherical	$-4.72\ 10^{-3}$	$3.49\ 10^{-2}$	0.96	$2.98\ 10^{-2}$
Stable ($\alpha = 1.5$)	$1.13\ 10^{-2}$	$3.78\ 10^{-2}$	0.97	$4.95\ 10^{-2}$

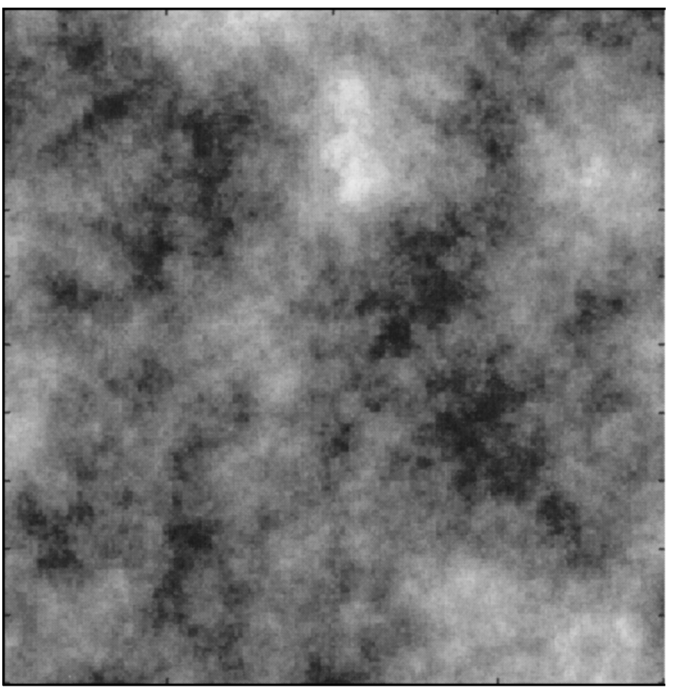

Figure 4. Two-dimensional isotropic Gaussian random field with spherical covariance (grid: 200 × 200 nodes; space step: 1; correlation length: 50; mean: 0; variance: 1).

Variable Uncoupling

We presented the separation between random numbers and structural parameters as an advantage. It implies that any of these numbers and parameters can be perturbed with no effect on the others. This feature confers great flexibility to the FFT-MA generator and is potentially of great interest to refine reservoir modeling.

It allows us to envision inversion processes inferring the structural parameters such as mean, variance, and correlation length, as well as the random numbers describing the permeability/porosity distributions.

Perturbing the Random Numbers

In this section, we propose to modify the random numbers. The convolution product introduced by the method of moving average involves a field z of uncorrelated random deviates. An independent random deviate is associated with each cell of the grid overimposed on the field. We assume that the covariance model is known: the Fourier transform G of its square root is calculated once and remains unchanged. A first realization is provided for a given z field. The following step consists in repeating the simulation for a field z' that derives from the perturbation of z. We can replace the values of z for all of the cells or only for some cells. In the case investigated here, we choose to draw new deviates for a selected region identified by a window in Figure 5. Running the simulation again produces a new realization. In order to boost the differences in the pictures, we apply the truncated Gaussian method (Galli and others, 1994) to the generated realizations. Then, the Gaussian field is turned into a facies field. For instance, in Figure 5 the reservoir is assumed to be constituted of two distinct facies with surface fractions 0.4 and 0.6.

In such conditions, both realizations respect the same covariance function. They look the same except where the normal deviates were modified. Actually, the truly modified area is larger than expected because of correlation effects. The cells at the border of the selected area are attributed new random deviates. They affect the field values in the grid cells as far as a correlation length. This drawback is also

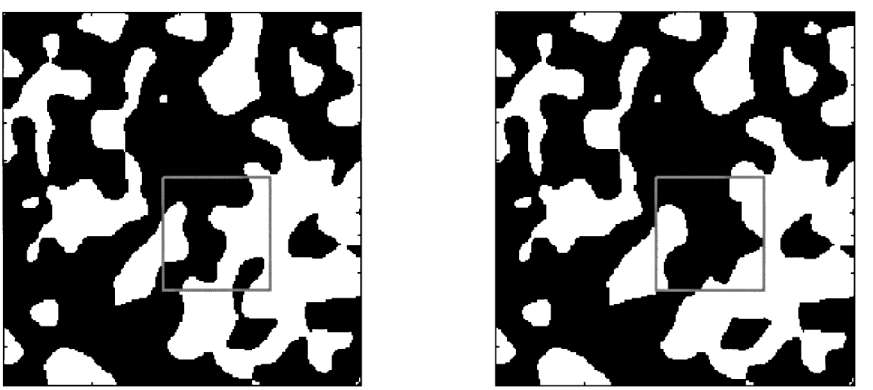

Figure 5. Two-dimensional isotropic truncated Gaussian random fields produced from identical normal deviates everywhere except in the window (grid: 200 × 200 nodes; space step: 1; covariance model: Gaussian; correlation length: 20; mean: 0; variance: 1; window size: 60 × 60 nodes).

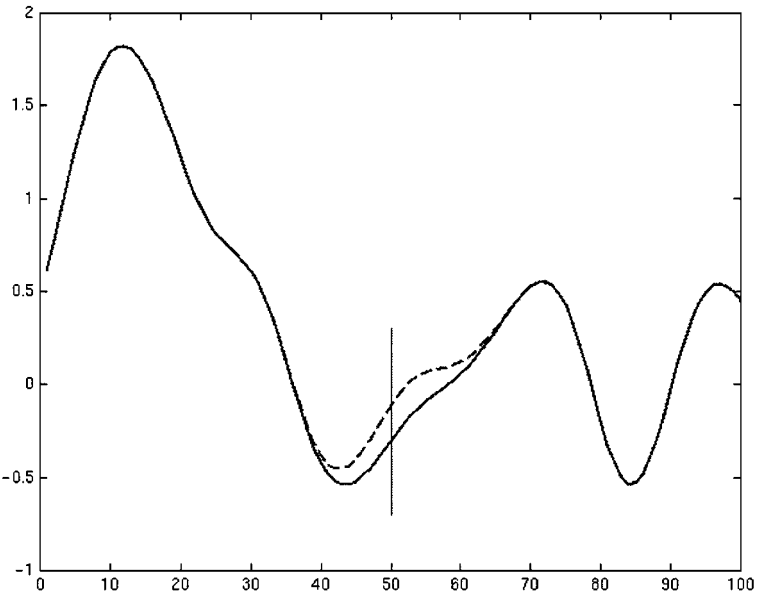

Figure 6. Comparison of a normal realization with a perturbed one. The perturbation is due to the variation in a single component of the underlying vector of independent normal deviates. (mean: 0; variance: 1; covariance model: Gaussian; correlation length: 30).

obvious in Figure 6. A one-dimensional realization with mean 0, variance 1 and a Gaussian covariance model is generated over the range [1 100] from an initial set of independent normal deviates z. The correlation length is 30. Then a single component of z is modified (the 50th one) and a new realization is simulated from the perturbed z. The input structural parameters are unchanged. Again, both realizations are similar except over the area centered at the perturbed point. The radius of this area roughly equals the correlation length. Actually, perturbing a single component of z involves changes over the whole field. However, the farther away the points are from the perturbed one, the smaller change there is in the simulated Gaussian field (Fig. 6). It can be noticed that when the local perturbation is restricted to a single point, the simulated Gaussian field is modified as if submitted to a pilot point (RamaRao and others, 1995).

Such an approach could be used to improve the efficiency of optimization algorithms as will be shown in the last section, because it generates perturbed realizations with all the same covariance. Thus, it is unnecessary to include a term into the objective function for matching a specified covariance as traditionally done (Deutsch and Cockerham, 1994). In addition, the FFT-MA algorithm makes it possible to update a reservoir study and refine the existing reservoir model. Indeed, newly obtained data could be accounted for through an optimization procedure

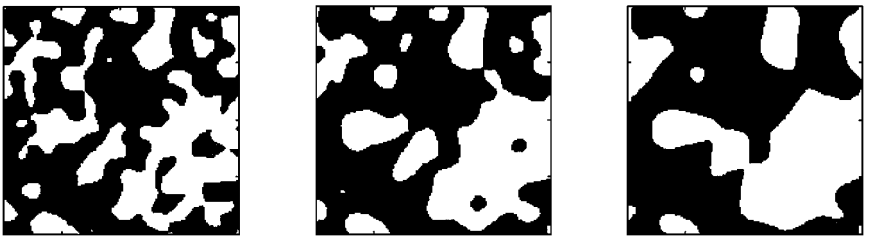

Figure 7. Two-dimensional isotropic truncated Gaussian random fields produced from identical normal deviates, and an increasing correlation length (grid: 200 × 200 nodes; space step: 1; covariance model: Gaussian; correlation length: 20–30–40, mean: 0; variance: 1; window size: 60 × 60 nodes).

perturbing the reservoir model only *locally*. The ability of the FFT-MA generator to produce locally modified realizations results from the use of the moving average method as the basic framework.

Perturbing the Structural Parameters

Let us focus on the structural parameters. In the following example (Fig. 7), we generate several realizations from identical input parameters, except the correlation length. The field of normal deviates, the mean and the variance are unchanged whereas we consider an increasing correlation length. Again, to make the figures simpler, we consider 2 facies with surface fractions 0.4 and 0.6. We notice that the general pattern is kept over the simulations. When the correlation length increases, heterogeneities tend to join to constitute largest heterogeneities. This result was expected because realizations are simulated from the same normal deviate field z.

This degree of freedom as for the structural parameters is of primary interest, because the measured data are usually insufficient to infer accurately the structural parameters. The structural parameters and the random numbers could be perturbed simultaneously in an optimization process.

Comparison with Other Methods

The properties described above are based upon the separation of the structural parameters from the random ones (i.e., the normal deviates). They are typical of moving average and Cholesky methods that involve independently a covariance kernel and a Gaussian white noise. First of all, they confer a great flexibility for conditioning realizations. Among the possible choices, we prefer the moving average method combined with the FFT algorithm. The decomposition of the covariance operator was shown to be straightforward in the discrete spectral domain and the convolution product in the space domain gets a simple product in the

spectral domain. As a result, using FFTs leads to fast and efficient generations of large stationary processes.

In this paragraph, we discard the advantages due to parameter uncoupling and compare the method described in this paper with referenced generators using FFTs (Gutjahr, 1989; Pardo-Iguzquiza and Chica-Olmo, 1993). The main difference depends on the way we work in the space and the spectral domains. In our case, we generate the independent random numbers in the space domain. On the contrary, the other FFT generators rely on the decomposition of the field into independent spectral components: the independent random numbers are generated in the spectral domain. This is of primary importance for conditioning. If we except the kriging method proposed by Gutjahr, Bullard, and Hatch (1997), to our knowledge the only conditioning procedure when using FFTs is due to Yao (1998). She performs conditioning fixing the spectral phases with a simulated annealing approach. The forward and backward discrete Fourier transforms imply that each of the space components is a linear combination of the spectral components. When fixing a single spectral component, she affects all the space components. The method that we presented is just the opposite because we propose to constrain the realization fixing the independent random components in the space domain. Conditioning a single random number has distinct meanings depending on the method. In the case of the approach developed by Yao (1998), it is associated with a perturbation of the whole field in the space domain. In our case, it corresponds to a local perturbation of the field in the space domain. Additionally, the FFT generator used by Yao (1998) is a "degenerate" version of the one introduced by Gutjahr (1989). The spectral components are built drawing phase shifts from a uniform distribution instead of real and imaginary parts from Gaussian distributions. Thus, this "degenerate" generator provides an approximation to a Gaussian field whereas the FFT-MA method gives a Gaussian random field.

NONLINEAR CONDITIONING

Stochastic Optimization Approach

Before running conditioning, it is worthwhile recalling what we want to achieve. Basically, an optimization procedure attempts to minimize an objective function that measures the misfit between a "true" model and a "guessed" one. It is formed from the weighted sum of the squared differences. Although Oliver, Cunha, and Reynolds (1997) stated that we should not try to produce legitimate conditional realizations by matching the covariance function exactly, several authors (Pérez, 1991; Deutsch, 1992; Gupta, 1992; Ouenes, 1992) suggested to include a term into the objective function for matching a specified covariance model. Minimizing the objective function is equivalent to reducing the misfit (1) between the production data calculated from the guessed model and the actual production

data and (2) between the covariance function (or variogram) calculated from the guessed model and the one inferred from the data (Deutsch and Journel, 1992). This approach hides a major difficulty: there is no simple way to estimate *a priori* the weight attributed to the covariance term in the objective function relative to the other kinds of data. Most of the time, this weight is just an empirical parameter.

In this paper, we assume that it is reasonable to generate Gaussian fields that match a selected covariance model. We suggest using the FFT-MA method to produce unconditional realizations and then to apply the gradual deformation rule (Hu, 2000) to perform conditioning. It allows us to perturb realizations while keeping them automatically consistent with the desired covariance function. The main consequence is that there is no need to include an additional term into the objective function for matching the covariance function. The gradual deformation method involves a smooth and continuous perturbation of an initial realization as a function of a parameter termed ρ. A variation in ρ provides a new realization still keeping the same spatial statistical characteristics. This perturbation method was used by Roggero and Hu (1998) to modify a Gaussian field y. These authors did not separate the random numbers from the structural parameters so that they could only consider the deformation of the entire y field with constant structural parameters. In our case, the gradual deformation method can be applied to modify all or some of the independent normal deviates z. Moreover, the structural parameters can be perturbed simultaneously.

Let us consider two sets of independent normal deviates randomly drawn and denoted z_1 and z_2, respectively. A new set of independent normal deviates z is built on the basis of the gradual deformation relation (Hu, 2000):

$$z = z_1 \cos(\pi\rho) + z_2 \sin(\pi\rho)$$

The structural parameters are assumed to be known and used to identify G. Let us note Z the Fourier transform of z. Introducing the inverse Fourier transform of $G \cdot Z$ into Equation (4) provides a new realization. Conditioning to production data is performed by estimating the parameter ρ that minimizes the objective function. As explained above, this objective function depends only on well data. Distinct optimization algorithms can be implemented to identify at least a local minimum of the objective function. In the example presented in the following section, we use the golden section search method that is appropriate for one-dimensional problems. The last iteration of the optimization process provides an "optimal" ρ—that is, an "optimal" set of independent normal deviates z.

However, considering only the realization chain built from z_1 and z_2 would limit the way we investigate the space of possible normal deviate sets. As a result, we create a sequence of several similar chains. Each chain is the basis of an optimization problem: an "optimal" z must be characterized from z_1 and z_2. The "optimal" z identified at the end of the optimization problem i is used as input

data in place of z_1 in the optimization problem $i+1$. A new set of independent normal deviates is generated in place of z_2 for each new chain. Finally, the sequence supplies the user with an "optimal" z.

If the structural parameters were unknown, the followed approach would be very similar. We would still consider a sequence of optimization problems. However, instead of changing only the normal deviates, we would also modify the parameters defining G (and mean m if necessary) into the optimization problem and from an optimization problem to the following one.

In this paper, we focus on the spatial continuity of the realizations of ergodic random functions. The ensemble statistics—that is, the statistics over a set of realizations of an ergodic random function—depend on whether the realizations are conditioned or not. However, the spatial statistics of these realizations are unchanged. As explained above, the conditional realizations are built so that they have the same spatial mean and covariance as the unconditional realizations. However, the ensemble moments change. This subject will be addressed more precisely in a future paper.

A Synthetic Example

In this last section, we focus on a synthetic example. Again to simplify visualization, we propose to produce facies maps constrained to geometric permeability averages. These averages are computed against radius from a center cell (Fig. 8).

Reference Realization

First we build a reference facies map (Fig. 9) discretized over a 50×50 grid. The size of a cell is 100×100 m. We selected a stable anisotropic variogram with an exponent $\alpha = 1.5$. Thus, the smoothness of the generated field is intermediate

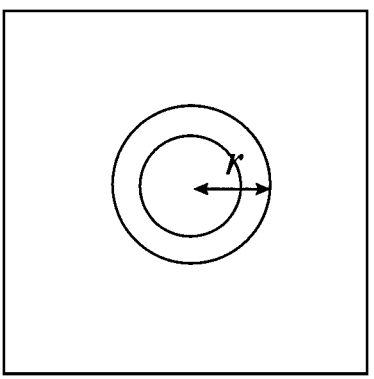

Figure 8. The average permeability is calculated for a centered growing area of radius r.

Table 2. Characteristics of the Facies

Facies	k (md)	Surface fraction	Color
1	100	0.40	Black
2	5	0.15	Gray
3	40	0.45	White

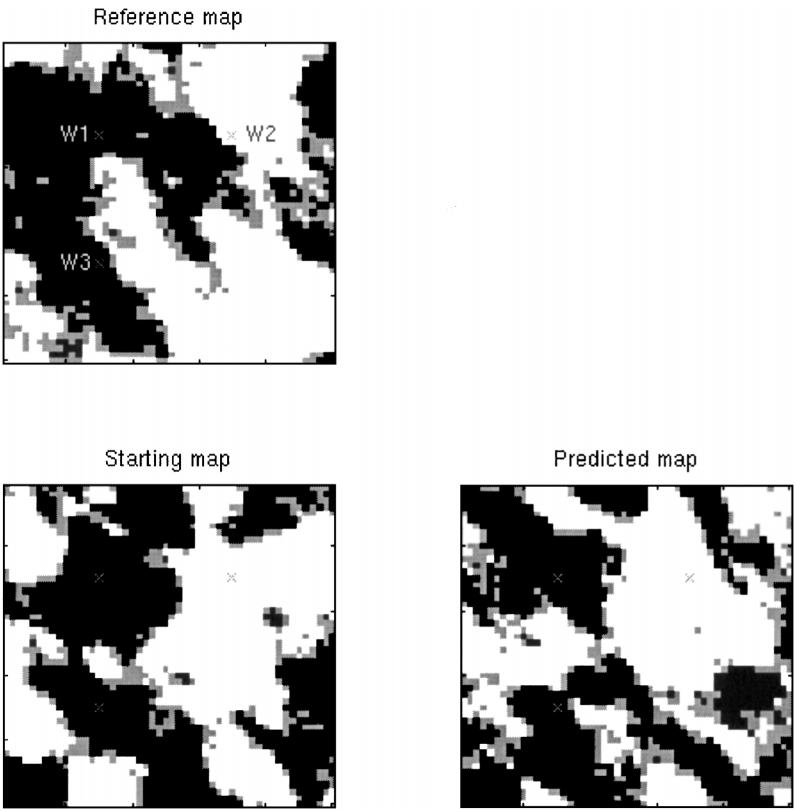

Figure 9. Facies map resulting from the optimization process compared to the reference and initial maps (the whole map is distorted).

between the exponential one ($\alpha = 1$) and the Gaussian one ($\alpha = 2$). The correlation lengths are 1500 m along the $(1, -1)$ axis and 1000 m along the orthogonal axis. As explained above, the truncated Gaussian method is applied to turn the continuous Gaussian field y into a three-facies field. The characteristics of the facies are reported in Table 2. We assume that three wells (W1, W2, and W3) are drilled into

the reservoir and reference geometric permeability averages are estimated for all of them against radius.

Primary Reservoir Study

At this point, we forget everything about the reference reservoir, except the structural parameters and the reference average permeabilities. Our purpose is to produce a realization that allows us to duplicate the reference data. In other words, we want to generate a set of normal deviates z that provide a facies map constrained to the reference geometric permeability averages. Basically, we consider a starting guess z_1 (Fig. 9) and apply the deformation method combined within an optimization sequence as described in the previous section. In addition, all the generated realizations are conditioned to the facies observed in W1, W2, and W3. As for parameter ρ, it affects all of the normal deviates z_1 (and z_2). The optimization for each realization chain is dedicated to the minimization of the objective function against ρ (Fig. 10). The final optimization results in a predicted facies map (Fig. 9) for which we calculate the geometric permeability averages centered in W1, W2, and W3. Those are compared to the reference geometric permeability averages (Fig. 11). We observe that the predicted data are consistent with the reference ones, especially for W1 and W3.

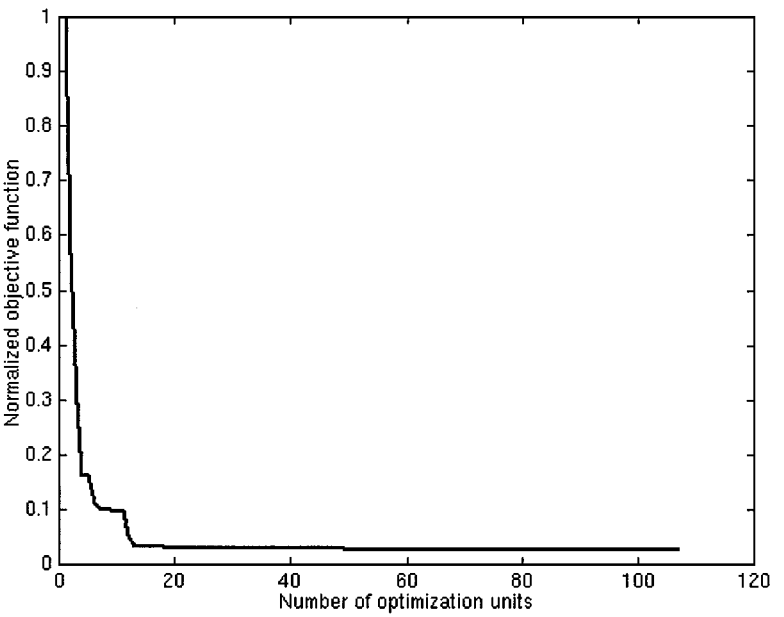

Figure 10. Normalized objective function against the number of optimization units when matching the data for W1, W2, and W3.

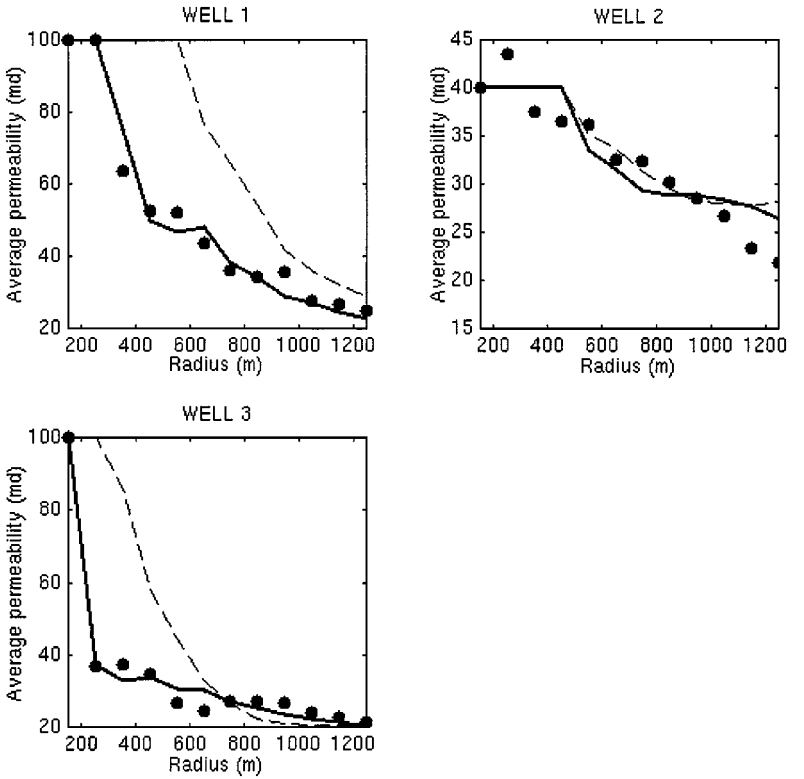

Figure 11. Comparison for W1, W2, and W3 of the reference geometric permeability averages (black circles) with those calculated for the starting map (dashed lines) and the predicted one (solid lines).

Updated Reservoir Study

Now, we assume that a new well, termed W4 (Fig. 12), is completed so that additional geometric permeability averages are available. We aim at updating the facies map predicted from the first study by integrating the new data. An optimization sequence similar to the previous one is run again providing an updated predicted map (Fig. 12). The starting realization for this second characterization study differs slightly from the previously predicted realization around well W4 (Fig. 9). So far, the predicted realization was not constrained to the reference facies at well W4. Compared to the primary characterization study, a difference deserves to be pointed out. In this case, we do not perturb all the normal deviates, but only the ones located in the right part of the map. As a result, average permeabilities first predicted for W1 and W3 are preserved. On the right side, the facies distribution is modified sequentially so that the objective function measuring the misfit between

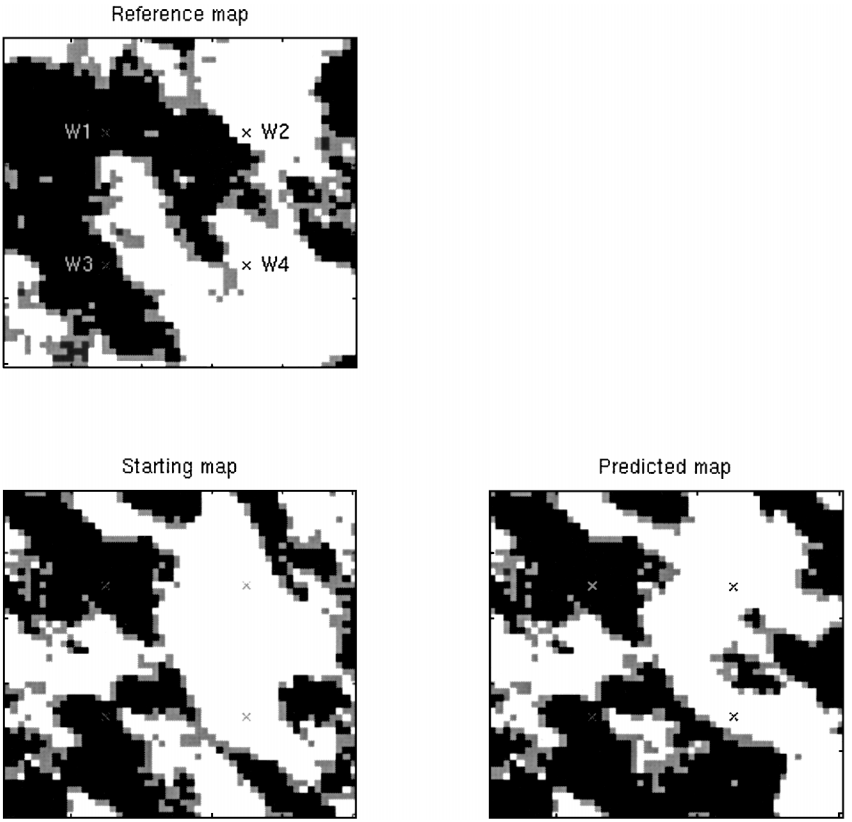

Figure 12. Facies map resulting from the optimization process compared to the reference and initial maps (only the right side of the map is distorted).

the reference and predicted data for W2 and W4 decreases (Fig. 13). Only the area around W4 could have been changed, but Figure 11 outlines that the agreement between the reference and calculated data for W2 was not so good. That is the reason why we perturb the normal deviates within all the right side of the map. The resulting average permeabilities are consistent with the reference ones (Fig. 14).

CONCLUSIONS

We want to emphasize that the FFT-MA generator is fast and flexible.

1. It is fast for producing unconditional realizations. Generating a random field over about 10^6 cells requires a dozen of seconds with a Sun station (Ultra Sparc 30).

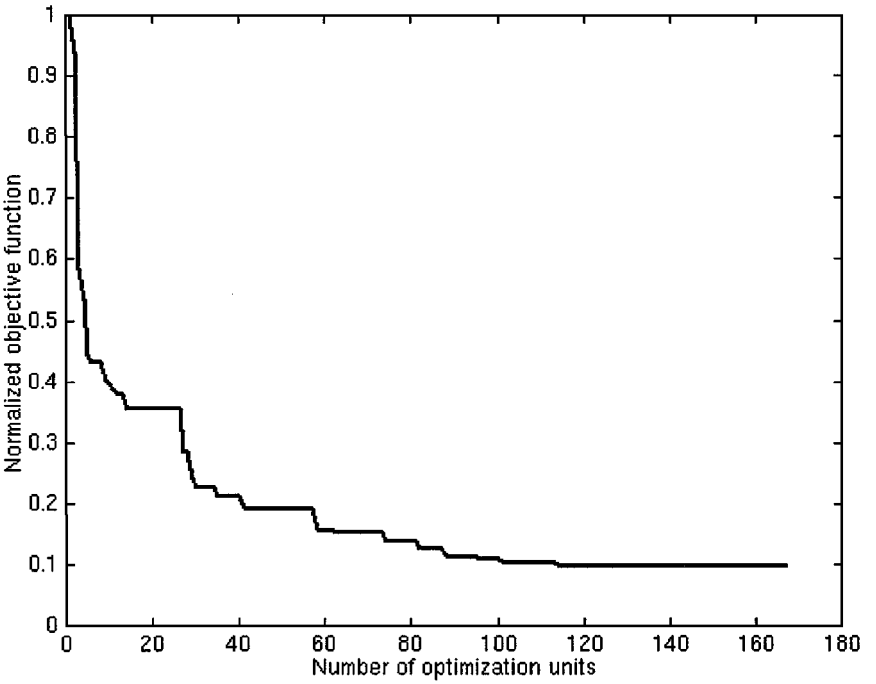

Figure 13. Normalized objective function against the number of optimization units when matching the data for W3 and W4.

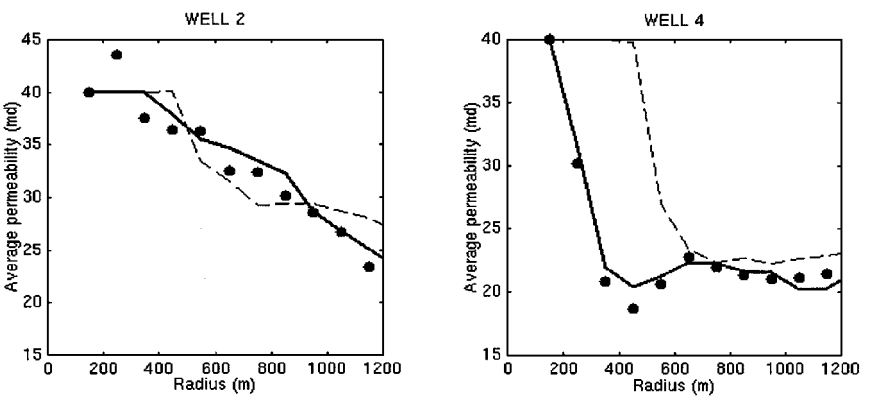

Figure 14. Comparison for W3 and W4 of the reference geometric permeability averages (black circles) with those calculated for the starting map (dashed lines) and the predicted one (solid lines).

2. The Fourier transform of $g * z$ is calculated easily. We no longer need to compute the square root of the covariance operator as well as the convolution product in the space domain.
3. It uncouples the random numbers (identified as the normal deviates) from the structural parameters. This property implies several advantages when performing optimization. First, it is no longer necessary to introduce an additional term into the objective function for matching the variogram because only realizations consistent with the desired variogram are built. Second, all or only some of the normal deviates can be perturbed so that the realization can be distorted only in selected areas. The ability to perform a local perturbation is new compared to the conventional spectral generators. Last, the random parameters can be modified, but also the structural ones so that a general inversion procedure can be envisioned (Le Ravalec, Hu, and Noetinger, 1999).

ACKNOWLEDGMENTS

This work was funded by the joint research project in reservoir engineering between Elf Exploration Production and the Institut Français du Pétrole.

REFERENCES

Alabert, F., 1987, The practice of fast conditional simulations through the LU decomposition of the covariance matrix: Math. Geology, v. 19, no. 5, p. 369–386.

Blanc, G., Touati, M., and Hu, L., 1998, Geostatistical modelling of fluid flow on flexible grids: 6th ECMOR Proceedings, 8–11 Sept., Peebles, Scotland, C30.

Bochner, S., 1936, Lectures on Fourier analysis: Princeton University Press, Princeton, NJ.

Chilès, J. P., 1995, Quelques méthodes de simulation de fonctions aléatoires intrinsèques: Cahiers de géostatistique, 5, p. 97–112.

Cooley, J. W., and Tukey, J. W., 1965, An algorithm for the machine computation of complex Fourier series: Math. Comp., v. 19, p. 297–301.

Davis, M. W., 1987, Production of conditional simulations via the LU triangular decomposition of the covariance matrix: Math. Geology, v. 19, no. 2, p. 91–98.

Deutsch, C. V., 1992, Annealing techniques applied to reservoir modeling and the integration of geological and engineering (well test) data: Unpublished doctoral dissertation, Stanford University, Stanford, CA, 325 p.

Deutsch, C. V., and Cockerham, P. W., 1994, Geostatistical modeling of permeability with annealing cosimulation (ACS): SPE 69th Annual Technical Conference and Exhibition, New Orleans, LA, p. 523–532.

Deutsch, C. V., and Journel, A. G., 1992, GSLIB: Geostatistical software library and user's guide: Oxford University Press, New York, 340 p.

Galli, A., Beucher, H., Le Loc'h, G., and Doligez, B., 1994, The pros and the cons of the truncated Gaussian method, *in* Armstrong, M., and Dowd, P. A., eds., Geostatistical simulations: Kluwer Academic Publishers, Dordrecht, The Netherlands, p. 217–233.

Gomez-Hernandez, J. J., and Journel, A. G., 1992, Joint sequential simulation of multiGaussian fields, *in* Soares, eds., Proceedings of the 4th International Geostatistical Congress: Kluwer Publishers, Troia, p. 85–94.

Gupta, A. D., 1992, Stochastic heterogeneity, dispersion, and field tracer response: Unpublished doctoral dissertation, University of Texas, Austin, TX, 248 p.

Gutjahr, A., 1989, Fast Fourier transforms for random field generation: New Mexico Tech. Project Report, NM, 106 p.

Gutjahr, A., Bullard, B., and Hatch, S., 1997, General joint simulations using a fast Fourier transform method: Math. Geology, v. 29, p. 361–389.

Hu, L. Y., 2000, Gradual deformation and iterative calibration of Gaussian-related stochastic models: Math. Geology, v. 32, no. 1, p. 87–108.

Johnson, M. E., 1987, Multivariate statistical simulations: John & New York, Wiley & Sons, 230 p.

Journel, A. G., 1974, Geostatistics for conditional simulation of ore bodies: Econ. Geology, v. 69, p. 673–687.

Journel, A. G., and Huijbregts, C. J., 1978, Mining geostatistics: Academic, San Diego, CA.

Lantuéjoul, C., 1994, Non conditional simulation of stationary isotropic multiGaussian random functions, *in* M. Armstrong, M., and Dowd, P. A., eds., Geostatistical simulations: Kluwer Academic Publishers, Dordrecht, The Netherlands, p. 147–177.

Le Ravalec, M., Hu, L. Y., and Noetinger, B., 1999, Stochastic reservoir modeling constrained to dynamic data: Local calibration and inference of the structural parameters: SPE Annual Technical Conference and Exhibition, Houston, TX, SPE 56556.

Mantoglou, A., 1987, Digital simulation of multivariate two- and three-dimensional stochastic processes with a spectral turning band method: Math. Geology, v. 19, no. 2, p. 129–149.

Mantoglou, A., and Wilson, J., 1982, The turning bands method for simulation of random fields using line generation by a spectral method: Water Resources Res., v. 18, p. 1379–1394.

Matheron, G., 1973, The intrinsic random functions and their applications: Adv. Appl. Prob., v. 5, p. 439–468.

Oliver, D. S., 1995, Moving averages for Gaussian simulation in two and three dimensions: Math. Geology., v. 27, no. 8, p. 939–960.

Oliver, D. S., Cunha, L. B., and Reynolds, A. C., 1997, A Markov chain Monte Carlo method of conditional simulation: Math. Geology, v. 29, no. 1, p. 61–91.

Ouenes, A., 1992, Application of simulated annealing to reservoir characterization and petrophysic inverse system: Unpublished Doctoral dissertation, New Mexico Technical, Socorro, NM, 205 p.

Pardo-Iguzquiza, E., and Chica-Olmo, M., 1993, The Fourier integral method: An efficient spectral method for simulation of random fields: Math. Geology, v. 25, no. 2, p. 177–217.

Pérez, G., Stochastic conditional simulation for description of reservoir properties: Unpublished doctoral dissertation, University of Tulsa, Tulsa, OK, 245 p.

Priestley, M. B., 1981, Spectral analysis and time series: Academic Press, London, GB.

RamaRao, B. S., La Venue, A. M., de Marsilly, G., and Marietta, M. G., 1995, Pilot point methodology for automated calibration of an ensemble of conditionally simulated transmissivity field: 1. Theory and computational experiments: Water Resources Res., v. 31, no. 3, p. 475–493.

Roggero, F., and Hu, L., 1998, Gradual deformation of continuous geostatistical models for history matching: SPE Annual Technical Conference and Exhibition, New Orleans, LA, SPE 49004.

Shinozuka, M., and Jan, C. M., 1972, Digital simulation of random processes and its applications: Jour. Sounds Vib., 25, no. 1, p. 111–128.

Yao, T., 1998, Conditional spectral simulation with phase identification: Math. Geology, v. 30, no. 3, p. 285–308.